ARTICLE IN PRESS

Journal of Computational and Applied Mathematics ▮ (▮▮▮▮) ▮▮▮–▮▮▮

Contents lists available at ScienceDirect

Journal of Computational and Applied Mathematics

journal homepage: www.elsevier.com/locate/cam

Numerical modeling of drop coalescence in the presence of soluble surfactants

I. Bazhlekov *, D. Vasileva

Institute of Mathematics and Informatics, Bulg. Acad. Sci, Acad. G. Bonchev str., bl.8, 1113 Sofia, Bulgaria

ARTICLE INFO

Article history:
Received 9 December 2014
Received in revised form 16 March 2015

Keywords:
Boundary integral method
Finite difference method
Drop coalescence
Film drainage
Soluble surfactant
Marangoni stress

ABSTRACT

The paper presents a numerical method for simulation of the effect of a soluble surfactant on the last stage of the drop coalescence (film formation, drainage and rupture). An axisymmetric interaction between drops is studied at small capillary and Reynolds numbers and small surfactant concentrations. The hydrodynamic part of the mathematical model includes the Stokes equations in the drop phase and their lubrication approximation in the gap between the drops (film phase), coupled with velocity and stress boundary conditions at the interfaces. The surfactant is considered soluble in both (drop and film) phases and the distribution of the surfactant concentration is governed by a convection–diffusion equation. A convection–diffusion equation is also used to model the distribution of the surfactant on the interfaces. The concentration in both phases is coupled with that on the interfaces via the adsorption isotherm and the fluxes between the interface and the bulk phases. The hydrodynamic and concentration parts of the mathematical model are related via the advection of the surfactant in the fluid phases and on the interfaces. On the other hand, a non-uniform surfactant concentration on the interfaces leads to a gradient of the interfacial tension which in turn leads to an additional tangential stress on the interfaces (Marangoni effects). For the flow in the drops a simplified version of Boundary integral method is used. Finite difference method is used for the flow in the gap, the position of the interfaces and the distribution of surfactant concentration on the interfaces, as well as in the fluid phases. Different approaches are used for an optimization of the numerical algorithm: Non-uniform meshes for space discretization in both (r and z) directions; Explicit and implicit first and second order time integration schemes with automatically adaptive time steps; A multiple time step integration scheme that can decrease significantly the computational time without loss of accuracy. Tests and comparisons are performed in order to investigate the accuracy and stability of the different numerical schemes.

1. Introduction

Drop coalescence is important to many natural and man made processes. A typical example is the process of emulsification where as a result of mixing of immiscible fluids droplets of size of micrometers, or smaller, are dispersed in a liquid matrix, forming an emulsion. Emulsions are of practical importance for many industrial applications, e.g. food and paint production, composite materials, pharmaceutics, petroleum, etc. The main difficulty for investigation (experimental or theoretical) of the process, and the emulsions itself, is the presence of several scales: the mixer of scale of meters; the drops of

* Corresponding author.
E-mail addresses: i.bazhlekov@math.bas.bg (I. Bazhlekov), vasileva@math.bas.bg (D. Vasileva).

http://dx.doi.org/10.1016/j.cam.2015.04.013
0377-0427/

scale of micrometers; the film region (gap between the drops) with a thickness of order of nanometers. Recently population balance models (see, for example, [1,2]) were successfully used for studying of emulsification. To overcome the difficulties related with the different scales the different subprocesses are considered separately in these models: flow in the mixer; drop deformation and breakup; drop coalescence, including film formation, its drainage and finally film rupture. The process of droplet breakup can be well described theoretically [3], whereas modeling of the coalescence dynamics is more difficult. This is because the drop coalescence involves interaction of two drops/bubbles, formation and drainage of a relatively stable film of order of nanometers.

In the framework of the population balance models the coalescence of two drops can be split conceptually into three elements (see, for example, [4]):

1. The external flow field, governing the frequency, strength and duration of collisions;
2. The process of film formation and drainage;
3. The destabilization of the film by van der Waals and other intermolecular forces, leading to rupture.

The first element furnishes the initial and boundary conditions for the second, which in turn provides those for the third element.

While reasonable first approximations for the collision frequency, force and duration, as well as for the critical film-rupture thickness can be derived in many cases, film drainage is particularly sensitive to the details of the system concerned. Small tangential stresses exerted on the film by the dispersed phase or by interfacial tension gradients translate into large forces per film volume, which strongly affects drainage rates. In pure liquid–liquid systems, exhibiting constant interfacial tension, the only tangential stresses are those exerted by the dispersed phase, arising from the internal motion within the drops. Most practically occurring fluid–liquid dispersions, however, contain surface-active materials, either by accident or design, that can strongly affect the drop and bubble coalescence (see for example [5] and references therein). It has long been realized that this sensitivity derives from the fact that minor variations in interfacial/surface tension, associated with small variations in the surfactant concentration, produce additional tangential stresses that translate into significant forces per unit volume of the film, thereby modifying film drainage rates.

The present paper solves the fully coupled flow and interface equations governing drainage and rupture of the film between interacting drops, together with those governing the surfactant transport and interfacial tension, at the following assumptions:

(a) Axisymmetric drop approach, under a small constant interaction force (small deformation);
(b) A nonionic surfactant;
(c) A low surfactant concentration.

For a discussion about the limitations imposed by the above restrictions see [5].

Numerical solutions of the equations governing film drainage are available in the case of pure liquids [6–11]. The effect of insoluble surfactants is also investigated intensively: on the film drainage [12,5,13–15]; on the interaction between surfactant covered spherical drops [16,17]. The influence of inter-phase mass transfer on the film drainage is studied numerically in [18–20].

The primary objective of the present paper is to develop a numerical procedure for solving the fully coupled system of equations governing the hydrodynamics and the surfactant transport in both phases as well as on the interface. The present study is an extension of previous works, where surfactants soluble only in one of the phases are considered: in the film phase [21] or in the drop/dispersed phase [22].

In the following section, the equations governing the film drainage and rupture in the absence of surface active species are extended to incorporate the influence of a surfactant soluble in both phases. In Section 3 the mathematical model is written in terms of transformed variables, making use of the simplifications provided by the limitation to low surfactant concentrations and small deformation. The numerical method is presented in Section 4. It consists of finite-difference schemes: explicit for the film and the interfacial convection–diffusion equation and hybrid (explicit/implicit) for the equations governing the convection–diffusion in the drop and film phases. A boundary integral method is used for the Stokes equations in the drop phase. In Section 5, results are presented and discussed. Finally, the conclusions are presented in Section 6.

2. Mathematical formulation

We consider two drops of one and the same Newtonian liquid interacting along the line of their centers under a given interaction force or velocity in another immiscible Newtonian fluid, see Fig. 1. Here μ is the drop viscosity, $h(r,t)$ is the film thickness, t denotes time. The surfactant concentrations in the film and in the drop phase are $C(r,z,t)$ and $C_d(r,z,t)$ respectively. In the present paper the drops are considered to approach each other at specified velocity $V(t)$, which is adjusted during the drainage process to maintain a constant interaction force. The same procedure can, however, be used for time-dependent approach velocities, including force–time relationships representative of actual drop collisions.

The model is simplified by a number of approximations, which are valid in the limit of gentle collisions (film radius a is much smaller than drop radii R_i) and which have been discussed in [5]. In addition, the influence of both inertia and viscous normal stresses on the film flow and on the adjacent flow in the drops is supposed to be negligible—an approximation that

Please cite this article in press as: I. Bazhlekov, D. Vasileva, Numerical modeling of drop coalescence in the presence of soluble surfactants, Journal of Computational and Applied Mathematics (2015), http://dx.doi.org/10.1016/j.cam.2015.04.013

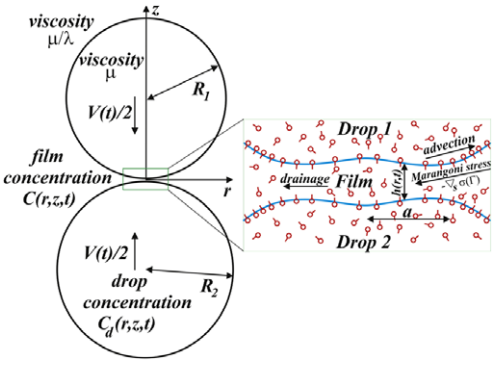

Fig. 1. Schematic sketch of the problem.

is generally acceptable when the drop coalescence is considered. In the regime of gentle collision ($a \ll R_i$) the governing equations are the same for unequal drops and equal drops when formulated in terms of the equivalent radius R_{eq} (see [4]):

$$R_{eq}^{-1} = \frac{1}{2}(R_1^{-1} + R_2^{-1}). \tag{1}$$

The mathematical model consists of hydrodynamic and surfactant transport models as described below.

2.1. Hydrodynamic part of the model

The lubrication approximation of the Stokes equations applies in the film in integral form:

$$\frac{\partial h}{\partial t} = -\frac{1}{r}\frac{\partial (rhu)}{\partial r}, \tag{2}$$

$$\tau = -\frac{h}{2}\frac{\partial p}{\partial r}, \tag{3}$$

where $0 < r < r_l$, h is the film thickness, τ the tangential stress exerted on the interface by the film, p is the pressure in the film. The mean velocity in the film u is sum of uniform and parabolic parts, u_u and u_p, respectively:

$$u = u_u + u_p = u_u - \frac{\lambda}{12\mu}h^2\frac{\partial p}{\partial r}. \tag{4}$$

Stokes equations apply in the drops:

$$-\nabla p_d + \mu\nabla^2\mathbf{u}_d = \mathbf{0}, \tag{5}$$

$$\nabla\cdot\mathbf{u}_d = 0, \tag{6}$$

where p_d is the pressure and $\mathbf{u}_d$ is the velocity in the drops.

The boundary conditions at the interfaces consist of continuity of tangential velocity and stress, together with a jump in normal stress associated with the interfacial tension σ:

$$u_u = (u_r)_d, \qquad \tau_d = \tau + \frac{\partial\sigma}{\partial r}, \tag{7}$$

$$p = \frac{2\sigma_{av}}{R_{eq}} - \frac{\sigma}{2}\left(\frac{\partial^2 h}{\partial r^2} + \frac{1}{r}\frac{\partial h}{\partial r}\right) + \frac{A}{6\pi h^3}, \tag{8}$$

where τ_d is the tangential stress exerted on the interface by the drop phase. The interfacial tension, σ, depends on r and t through the surfactant concentration $\Gamma(r,t)$, which will be discussed later; σ_{av} is an average value of σ. The last term is the disjoining pressure due to the van der Waals attractive force between the interfaces, where A is the Hamaker constant.

The outer boundary conditions are prescribed pressure and approach velocity at sufficiently large $r = r_l$:

$$p(r_l) = 0, \qquad \left(\frac{\partial h}{\partial t}\right)_{r_l} = V(t), \tag{9}$$

where $V(t)$ is adjusted so that:

$$2\pi\int_0^{r_l}\left(p - \frac{A}{6\pi h^3}\right) r\,dr = F = \frac{2\pi a^2\sigma_{av}}{R_{eq}} = \text{const}, \tag{10}$$

F is the interaction force and is chosen to be constant; a is a measure of the film radius ($a = \text{const}$).

Please cite this article in press as: I. Bazhlekov, D. Vasileva, Numerical modeling of drop coalescence in the presence of soluble surfactants, Journal of Computational and Applied Mathematics (2015), http://dx.doi.org/10.1016/j.cam.2015.04.013

Additionally, the film velocities u_r and u_z are necessary in the surfactant transport model. They are given by:

$$u_r = u_u + \frac{\lambda}{2\mu}\frac{\partial p}{\partial r}\left(z^2 - \left(\frac{h}{2}\right)^2\right), \tag{11}$$

$$u_z = -\frac{1}{r}\frac{\partial (r u_u z)}{\partial r} - \frac{\lambda}{2r\mu}\frac{\partial}{\partial r}\left[r\frac{\partial p}{\partial r}\left(\frac{z^3}{3} - \frac{h^2}{4}z\right)\right], \tag{12}$$

where $0 < z < h(r)/2$ in the film and u_z is obtained from the continuity equation. We set $z_d = z - h(r)/2$ and thus $z_d > 0$ in the drop phase. Further we will consider the interface between the film and drops as flat in the drop phase.

2.2. Surfactant transport model

The following convection–diffusion equations, which govern the surfactant distribution in both phases (film and drop) and on the interfaces (related with Marangoni effect) are incorporated into the model.

At the interface

$$\frac{\partial \Gamma}{\partial t} + \frac{1}{r}\frac{\partial (r\Gamma u_u)}{\partial r} - \frac{D_s}{r}\frac{\partial}{\partial r}\left(r\frac{\partial \Gamma}{\partial r}\right) = j_s + (j_s)_d, \tag{13}$$

where $\Gamma(r,t)$ is the surfactant concentration on the interface, D_s is the surface diffusion and the surfactant fluxes at the interface, j_s and $(j_s)_d$, are given by Fick's law:

$$j_s = -D(n.\nabla C)|_{z=h/2} = -D\left(\frac{\partial C}{\partial z} - \frac{\partial h}{\partial r}\frac{\partial C}{\partial r}\right)\Big|_{z=h/2}, \qquad (j_s)_d = D_d\left(\frac{\partial C_d}{\partial z_d}\right)\Big|_{z_d=0}, \tag{14}$$

where D and D_d are the bulk diffusion coefficients in the film and in the drops, respectively. Boundary conditions of symmetry at $r = 0$ and uniform surfactant distribution at large $r = r_l$ are respectively:

$$\left(\frac{\partial \Gamma}{\partial r}\right)_{r=0} = 0; \qquad \left(\frac{\partial \Gamma}{\partial r}\right)_{r=r_l} = 0. \tag{15}$$

The dependence of the interfacial tension $\sigma(\Gamma)$ on the surfactant concentration is given by the 2D gas law:

$$\sigma_s - \sigma = \Gamma R_G T, \tag{16}$$

where R_G is the gas constant, T the absolute temperature and σ_s the interfacial tension in absence of a surfactant.

In the film

The surfactant concentration $C(r,z)$ in (14) is governed by the convection–diffusion equation in the film:

$$\frac{\partial C}{\partial t} + u_r\frac{\partial C}{\partial r} + u_z\frac{\partial C}{\partial z} = D\left(\frac{\partial^2 C}{\partial z^2} + \frac{1}{r}\frac{\partial}{\partial r}\left(r\frac{\partial C}{\partial r}\right)\right). \tag{17}$$

Boundary conditions of symmetry at $r = 0$, $z = 0$ and uniform surfactant distribution at large $r = r_l$ are respectively:

$$\left(\frac{\partial C}{\partial r}\right)_{r=0} = 0, \qquad \left(\frac{\partial C}{\partial z}\right)_{z=0} = 0, \qquad \left(\frac{\partial C}{\partial r}\right)_{r=r_l} = 0. \tag{18}$$

The boundary condition at the interfaces is given by the linear adsorption isotherm, relating the surfactant concentration in the film with that on the interface, where K is the adsorption parameter:

$$KC(r, z = h/2, t) = \Gamma(r,t). \tag{19}$$

In the drops

The surfactant concentration $C_d(r,z)$ in the drops is governed by the convection–diffusion equation:

$$\frac{\partial C_d}{\partial t} + (u_r)_d\frac{\partial C_d}{\partial r} + (u_{z_d})_d\frac{\partial C_d}{\partial z_d} = D_d\left(\frac{\partial^2 C_d}{\partial z_d^2} + \frac{1}{r}\frac{\partial}{\partial r}\left(r\frac{\partial C_d}{\partial r}\right)\right). \tag{20}$$

Boundary conditions of symmetry at $r = 0$ and uniform surfactant distribution at large $r = r_l$ and $z_d = \infty$ are respectively:

$$\left(\frac{\partial C_d}{\partial r}\right)_{r=0} = 0, \qquad \left(\frac{\partial C_d}{\partial z_d}\right)_{z_d=\infty} = 0, \qquad \left(\frac{\partial C_d}{\partial r}\right)_{r=r_l} = 0. \tag{21}$$

The boundary condition at the interfaces is given by the linear adsorption isotherm, relating the surfactant concentration in the drops with that on the interface, where K_d is the adsorption parameter:

$$K_d C_d(r, z_d = 0, t) = \Gamma(r,t). \tag{22}$$

Please cite this article in press as: I. Bazhlekov, D. Vasileva, Numerical modeling of drop coalescence in the presence of soluble surfactants, Journal of Computational and Applied Mathematics (2015), http://dx.doi.org/10.1016/j.cam.2015.04.013

2.3. Initial conditions

The initial condition for the film thickness corresponds to undeformed drops (the pressure $p = 0$):

$$h(r, t = 0) = h_{ini} + \frac{r^2}{R_{eq}}. \tag{23}$$

For the surfactant concentrations Γ at the interface, C in the film, and C_d in the drops two limiting non-equilibrium initial distributions are considered:

- Initially uniform surfactant distribution in the film and on the interfaces. The drop phase is clean of surfactant:

$$\begin{aligned} &\Gamma(r, t = 0) = \Gamma_{ini} = KC(r, z, t = 0) = KC_{ini} = \text{const};\\ &C_d(r, z_d, t = 0) = C_{d,ini} = 0. \end{aligned} \tag{24}$$

- Initially uniform surfactant distribution in the drops and on the interfaces. The film (continuous) phase is clean of surfactant:

$$\begin{aligned} &\Gamma(r, t = 0) = \Gamma_{ini} = K_d C_d(r, z_d, t = 0) = K_d C_{d,ini} = \text{const};\\ &C(r, z, t = 0) = C_{ini} = 0. \end{aligned} \tag{25}$$

2.4. Transformation and dimensionless parameters

A simplification of the governing equations is possible via a transformation of the variables that renders them dimensionless and reduces the number of parameters. The transformation is:

$$\begin{aligned} &t^* = \frac{t\sigma_s a'}{R_{eq}\mu}; \quad r^* = \frac{r}{R_{eq}a'}; \quad z^* = \frac{z}{R_{eq}a'^2}; \quad h^* = \frac{h}{R_{eq}a'^2}; \quad \tau^* = \frac{\tau R_{eq}}{\sigma_s a'}; \quad p^* = \frac{pR_{eq}}{\sigma_s};\\ &u_r^* = \frac{u_r\mu}{\sigma_s a'^2}; \quad u_z^* = \frac{u_z\mu}{\sigma_s a'^3}; \quad \Gamma^* = \frac{\Gamma R_G T}{\sigma_s a'^2}; \quad C^* = \frac{CR_G TR_{eq}}{\sigma_s}; \quad C_d^* = \frac{C_d R_G TR_{eq}}{\sigma_s a'^2};\\ &z_d^* = \frac{z_d}{R_{eq}a'}; \quad (u_r)_d^* = \frac{(u_r)_d\mu}{\sigma_s a'^2}; \quad (u_z)_d^* = \frac{(u_z)_d\mu}{\sigma_s a'^2}; \quad \tau_d^* = \frac{\tau_d R_{eq}}{\sigma_s a'}; \quad p_d^* = \frac{p_d R_{eq}}{\sigma_s a'}, \end{aligned} \tag{26}$$

where a' is the dimensionless radius of the film, $a' = a/R_{eq}$. The dimensional film radius a is given by the condition of the constant interaction force, Eq. (10). In the small deformation limit (gentle collisions), considered here, the parameter a' is small ($a' \ll 1$). Note that the dispersed-phase variables z_d, $(u_z)_d$, C_d and p_d are seen to transform differently from their continuous-phase counterparts.

Applying the transformation above, the parameters of the problem are reduced to 9 dimensionless groups:

$$\begin{aligned} &\lambda^* = \lambda a'; \quad K^* = \frac{K}{R_{eq}a'^2}; \quad K_d^* = \frac{K_d}{R_{eq}}; \quad Pe_s^* = \frac{\sigma_s R_{eq}a'^3}{D_s\mu}; \quad Pe^* = \frac{\sigma_s R_{eq}a'^5}{D\mu};\\ &Pe_d^* = \frac{\sigma_s R_{eq}a'^3}{D_d\mu}; \quad C_{ini}^* = \frac{C_{ini}R_G TR_{eq}}{\sigma_s}; \quad C_{d,ini}^* = \frac{C_{d,ini}R_G TR_{eq}}{\sigma_s a'^2}; \quad A^* = \frac{A}{4\pi\sigma_s R_{eq}^2 a'^2}; \end{aligned}$$

the viscosity ratio λ^*; the adsorption parameters K^* and K_d^*; Péclet numbers: Pe_s^* on the interface, Pe^* in the film, and Pe_d^* in the drops; the initial surfactant concentrations C_{ini}^* in the film, $C_{d,ini}^*$ in the drops and the transformed Hamaker parameter A^*.

3. Transformed equations

Applying transformation (26), we obtain the governing equations in dimensionless form:

3.1. Hydrodynamic part

Equations in the film, see (2), (3):

$$\frac{\partial h^*}{\partial t^*} = -\frac{1}{r^*}\frac{\partial(r^* h^* u_u^*)}{\partial r^*} + \frac{1}{r^*}\frac{\lambda^*}{12}\frac{\partial}{\partial r^*}\left(h^{*3} r^* \frac{\partial p^*}{\partial r^*}\right), \tag{27}$$

$$\tau^* = -\frac{h^*}{2}\frac{\partial p^*}{\partial r^*}, \tag{28}$$

with velocity (see (11), (12))

$$u_r^* = u_u^* + \frac{\lambda^*}{2}\frac{\partial p^*}{\partial r^*}\left(z^{*2} - \left(\frac{h^*}{2}\right)^2\right),$$

$$u_z^* = -\frac{1}{r^*}\frac{\partial(r^* u_u^* z^*)}{\partial r^*} - \frac{\lambda^*}{2r^*}\frac{\partial}{\partial r^*}\left[r^*\frac{\partial p^*}{\partial r^*}\left(\frac{z^{*3}}{3} - \frac{h^{*2} z^*}{4}\right)\right].$$

Please cite this article in press as: I. Bazhlekov, D. Vasileva, Numerical modeling of drop coalescence in the presence of soluble surfactants, Journal of Computational and Applied Mathematics (2015), http://dx.doi.org/10.1016/j.cam.2015.04.013

Equations in the drops, see (5), (6):

$$-\nabla^* p_d^* + \nabla^{*2}\mathbf{u}_d^* = \mathbf{0}, \quad \nabla^* \cdot \mathbf{u}_d^* = 0. \tag{29}$$

Boundary conditions at the interfaces, see (7):

$$u_u^* = (u_r^*)_d, \qquad \tau_d^* = \tau^* - \frac{\partial \Gamma^*}{\partial r^*}. \tag{30}$$

The 2D gas law, Eq. (16), can be written in dimensionless form as:

$$\sigma^* = 1 - a'^2 \Gamma^*, \tag{31}$$

where $\sigma^* = \sigma/\sigma_s$. Thus the jump in the normal stress (see (8) and Eq. (8) of [21]) in dimensionless form can be approximated with an error $O(a'^2)$ as:

$$p^* = 2 - \frac{1}{2}\left(\frac{\partial^2 h^*}{\partial r^{*2}} + \frac{1}{r^*}\frac{\partial h^*}{\partial r^*}\right) + \frac{2A^*}{3h^{*3}}. \tag{32}$$

The outer boundary conditions (see (9), (10)):

$$p^*(r_l^*) = 0, \qquad \left(\frac{\partial h^*}{\partial t^*}\right)_{r_l^*} = V^*(t^*), \qquad \int_0^{r_l^*}\left(p^* - \frac{2A^*}{3h^{*3}}\right) r^*\, dr^* = 1. \tag{33}$$

3.2. Surfactant transport model

At the interface, see (13)–(15):

$$\frac{\partial \Gamma^*}{\partial t^*} + \frac{1}{r^*}\frac{\partial (r^*\Gamma^* u_u^*)}{\partial r^*} - \frac{1}{Pe_s^* r^*}\frac{\partial}{\partial r^*}\left(r^*\frac{\partial \Gamma^*}{\partial r^*}\right) = \frac{1}{Pe_d^*}\left(\frac{\partial C_d^*}{\partial z_d^*}\right)\Big|_{z_d^*=0} - \frac{1}{Pe^*}\left(\frac{\partial C^*}{\partial z^*} - a'^2\frac{\partial h^*}{\partial r^*}\frac{\partial C^*}{\partial r^*}\right)\Big|_{z^*=h/2} \tag{34}$$

with boundary conditions:

$$\left(\frac{\partial \Gamma^*}{\partial r^*}\right)_{r^*=0} = 0, \qquad \left(\frac{\partial \Gamma^*}{\partial r^*}\right)_{r^*=r_l^*} = 0. \tag{35}$$

As $a'^2 \ll 1$, the last term in (34) will be further ignored.

Surfactant transport in the film, see (17)–(19):

$$\frac{\partial C^*}{\partial t^*} + u_r^*\frac{\partial C^*}{\partial r^*} + u_z^*\frac{\partial C^*}{\partial z^*} = \frac{1}{Pe^*}\left(\frac{\partial^2 C^*}{\partial z^{*2}} + \frac{a'^2}{r^*}\frac{\partial}{\partial r^*}\left(r^*\frac{\partial C^*}{\partial r^*}\right)\right), \tag{36}$$

with boundary conditions

$$\left(\frac{\partial C^*}{\partial r^*}\right)_{r^*=0} = 0, \qquad \left(\frac{\partial C^*}{\partial z^*}\right)_{z^*=0} = 0, \qquad \left(\frac{\partial C^*}{\partial r^*}\right)_{r^*=r_l^*} = 0, \tag{37}$$

$$K^* C^*|_{z^*=h^*/2} = \Gamma^*. \tag{38}$$

The last term in (36) will also be ignored further, as $a'^2 \ll 1$.

Surfactant transport in the drops, see (20)–(22):

$$\frac{\partial C_d^*}{\partial t^*} + (u_r^*)_d\frac{\partial C_d^*}{\partial r^*} + (u_z^*)_d\frac{\partial C_d^*}{\partial z_d^*} = \frac{1}{Pe_d^*}\left(\frac{1}{r^*}\frac{\partial}{\partial r^*}\left(r^*\frac{\partial C_d^*}{\partial r^*}\right) + \frac{\partial^2 C_d^*}{\partial z_d^{*2}}\right) \tag{39}$$

with boundary conditions

$$\left(\frac{\partial C_d^*}{\partial r^*}\right)_{r^*=0} = \left(\frac{\partial C_d^*}{\partial z_d^*}\right)_{z_d^*=z_\infty^*} = \left(\frac{\partial C_d^*}{\partial r^*}\right)_{r^*=r_l^*} = 0, \tag{40}$$

where z_∞^* is sufficiently large and

$$K_d^* C_d^*|_{z_d^*=0} = \Gamma^*. \tag{41}$$

3.3. Initial conditions, see (23)–(25)

For the film thickness:

$$h^*(r^*, t^* = 0) = h_{ini}^* + r^{*2}. \tag{42}$$

Please cite this article in press as: I. Bazhlekov, D. Vasileva, Numerical modeling of drop coalescence in the presence of soluble surfactants, Journal of Computational and Applied Mathematics (2015), http://dx.doi.org/10.1016/j.cam.2015.04.013

For the surfactant concentrations:

$$\Gamma^*(r^*, t^* = 0) = \Gamma^*_{ini} = K^* C^*(r^*, z^*, t^* = 0) = K^* C^*_{ini} = \text{const};$$
$$C^*_d(r^*, z^*_d, t^* = 0) = C^*_{d,ini} = 0. \tag{43}$$

or

$$\Gamma^*(r^*, t^* = 0) = \Gamma^*_{ini} = K^*_d C^*_d(r^*, z^*_d, t^* = 0) = K^*_d C^*_{d,ini} = \text{const};$$
$$C^*(r^*, z^*, t^* = 0) = C^*_{ini} = 0. \tag{44}$$

4. Numerical scheme

The scheme for numerical solution of the mathematical model described in the previous section is as follows: Starting from a given $h^*(r^*, t^*)$ and Γ^*, given initially by (42)–(44), then p^* is calculated from (32) and τ^*_d from (28), providing (via the second equation in (30), where the Marangoni effect is taken into account) a boundary condition for the Stokes equations (29). The solution of these equations in the drop then gives u^*_u via (30). Now, having u^*_u and p^*, the solution at the next time step is obtained: for the film thickness from (27) and for the surfactant concentration Γ^* on the interface via Eq. (34). The surfactant concentration in the film C^* and in the drops C^*_d at the next time step is calculated from Eqs. (36) and (39) respectively, where the boundary conditions at the interface ($C^*(r^*, z^* = h^*/2, t^*)$ and $C^*_d(r^*, z^*_d = 0, t^*)$) are given by the surfactant concentration Γ^* via (38) and (41). Thus, the whole process can be repeated. The prescribed interaction force in (33) is satisfied using the same approach as in [5].

Eqs. (29), governing the flow in the drops, are solved by a boundary integral method, approximating the interface as flat and neglecting the normal velocity at the interface. The velocity in the drops is given in [22] (see also [23,24])

$$(u^*_r)_d = \int_0^{r^*_l} \phi_1(r^*, r')\tau_d(r')\, dr', \qquad (u^*_{z_d})_d = \int_0^{r^*_l} \phi_3(r^*, r')\tau_d(r')\, dr',$$

where

$$\phi_1(r^*, r') = \frac{r'}{4\pi}\int_0^{2\pi}\left(\frac{2\cos\theta}{(r^{*2} + r'^2 - 2r^*r'\cos\theta + z^{*2}_d)^{1/2}} - \frac{z^2_d\cos\theta + r^*r'\sin^2\theta}{(r^{*2} + r'^2 - 2r^*r'\cos\theta + z^{*2}_d)^{3/2}}\right) d\theta \tag{45}$$
$$\phi_3(r^*, r') = \frac{r'}{4\pi}\int_0^{2\pi}\frac{(r^*\cos\theta - r')z^*_d r'\, d\theta}{(r^{*2} + r'^2 - 2r^*r'\cos\theta + z^{*2}_d)^{3/2}}.$$

Special attention is paid to the singularity in formula (45), which appears at $r^* = r'$ and $z^*_d = 0$. It can be shown that the above solution for the velocity on the interface (at $z^* = 0$) is exactly the one given by (39–40) of [21].

Eq. (27), governing the evolution of the film thickness h^*, is a nonlinear, fourth-order partial differential equation with respect to h^*. To solve it, a Euler explicit scheme is used for the time integration in combination with a second order finite difference scheme for the discretization of the spatial derivatives. In practical applications the numerical simulations have to be able to follow evolution of the film with minimal thickness $h^*_{\min}$ down to order of 10^{-3}. This in fact requires two things: high accuracy of the calculations (of order 10^{-4}), and ability to cover a broad time interval ($t^* \in [0, t^*_l]$, where t^*_l could be of order 10^4), see Figs. 7 and 8. Another challenge is due to the stiffness of Eq. (27), as this is mentioned by other authors [25], especially for high values of λ^*. Thus here a special attention is paid to the space discretization and time integration of Eq. (27), based on an assessment for the stability of the Euler explicit scheme. It can be shown (see also [21]) that the requirements for numerical stability of Eq. (27) arising from the plug and parabolic parts of the flow (the two terms on the right-hand-side of (27)) as well as from the disjoining pressure (the last term of (32)) are respectively:

$$(\Delta t^*)_I \le \text{const}\cdot\min_{j\in[0,N]}\left(\frac{\Delta r^{*3}_j}{h^{*2}_j}\right); \qquad (\Delta t^*)_{II} \le \frac{24}{\lambda^*}\min_{j\in[0,N]}\left(\frac{\Delta r^{*4}_j}{h^{*3}_j}\right);$$
$$(\Delta t^*)_{III} \le \frac{6}{\lambda^* A^*}\min_{j\in[0,N]}\left(\Delta r^{*2}_j h^*_j\right), \tag{46}$$

where r_j, $j = 0, \ldots, N$, are the mesh nodes in the r direction, Δt^* is the time step, $\Delta r^*_j = r^*_j - r^*_{j-1}$ are the space steps, and $h^*_j = h^*(r^*_j)$ are the values of the film thickness h^* in the nodes r^*_j.

A simple analysis shows that the use of uniform discretization in the r^* direction (for instance $\Delta r^* \sim 10^{-2}$) will limit the time step ($(\Delta t^*)_{II}$) to values of order 10^{-14} ($h^*(r^*_l \sim 10) \sim 10^2$). To avoid such extremely small time steps, non-uniform meshes are generated depending on the values of h^*_j: small constant step Δr^*_f in the film region $0 < r^* < 1.2$, where the most severe deformation appears; increasing by geometrical-progression law steps at large r^*, becoming of order 1 at the end of the computational domain r^*_l. Thus the time steps Δt^* that satisfy the stability conditions (46), and are used in the present calculations, are in the interval 10^{-5}–10^{-6}.

Similar approach is used for discretization of the computational domain in the z^*_d direction in the drop phase and in the z^* direction in the film phase. Non-uniform meshes are used: small steps ($\Delta z^*_d \sim 0.01$) close to the interface $z^*_d = 0$ and relatively large steps ($\Delta z^*_d \sim 1$) at large z^*_d. The mesh in the z^* direction in the film is also non-uniform, an order of

Please cite this article in press as: I. Bazhlekov, D. Vasileva, Numerical modeling of drop coalescence in the presence of soluble surfactants, Journal of Computational and Applied Mathematics (2015), http://dx.doi.org/10.1016/j.cam.2015.04.013

magnitude finer close to the interface $z^* = h^*/2$ than in the center of the film $z^* = 0$. Additionally, the transformation $\eta = 2z^*/h^*(r^*, z^*, t^*)$ is applied in order to account for the curvilinear form of the interface, an approach used earlier by Saboni et al. [18].

Another optimization of the time integration is based on a qualitative comparison between the different parts of the hydrodynamic model (Eq. (27)), regarding the CPU time for their calculation and the restrictions on the time step that they impose. Thus the plug part of the film flow, u_u^*, depends on the flow in the drops via the first boundary condition in (30) and requires the solution of the Stokes equations (45) there. The second, parabolic part (second term on the r.h.s. of (4)), is computed directly via (32) and consumes much less CPU time. On the other hand the ratio $(\Delta t^*)_I/(\Delta t^*)_{II}$ is proportional to $\lambda^* h^*/\Delta r^*$ and can be of order 10^3–10^4. Based on the above comparisons a multiple time step approach is used (see [26]) with automatic choice of the time step. Thus the parabolic part of the film flow is calculated at every time step (Δt^*), that is chosen to satisfy the second and third restrictions in (46). The plug part of the film flow, u_u^*, is calculated via (45) once at every M such time steps. In this way the simulations are numerically stable and almost M times faster compared to the standard one, where single time step integration ($M = 1$) is used.

For the convection–diffusion equations in the drop and film phases, first order Euler explicit time integration scheme appeared to be numerically unstable. Thus, based on the fact that the gradients of the surfactant concentration are much higher in the z^* than in the r^* direction, a hybrid (explicit/implicit) method is developed for time integration of the convection–diffusion equations in the drop and film phases. It consists of explicit time integration in the r^* direction and implicit in the z^* (z_d^*) direction. In this scheme, N five-diagonal systems have to be solved (N is the number of nodes in the r^* direction) for each of the phases (drop and film). If we denote $C(i, j, k) = C^*(r_i^*, z_j^*, t_k^*)$ the hybrid explicit/implicit scheme for the film phase (Eq. (36)) can be written as:

$$C(i,j,k+1) + \beta\Delta T\left[u_z^*\delta_z - \frac{1}{Pe^*}\delta_z^2\right]C(i,j,k+1)$$
$$= C(i,j,k) - \Delta T u_r^*\delta_r C(i,j,k) + (\beta-1)\Delta T\left[u_z^*\delta_z - \frac{1}{Pe^*}\delta_z^2\right]C(i,j,k), \tag{47}$$

where $\Delta T = M\Delta t^*$; δ_x and δ_x^2 are finite difference approximations for the first and second derivatives with respect to the variable x (x stands for r^* or z^*). Here five node discretization is used for the first and second derivatives in the r^* and z^* directions. Thus the second derivative is approximated as:

$$\frac{\partial^2 C(i,j,k)}{\partial z^{*2}} \approx \delta_z^2 C(i,j,k) = a_1.C(i,j-2,k) + a_2.C(i,j-1,k)$$
$$+ a_3.C(i,j,k) + a_4.C(i,j+1,k) + a_5.C(i,j+2,k),$$

with $a_1 = y_1$, $a_2 = y_2$, $a_3 = -(y_1 + y_2 + y_3 + y_4)$, $a_4 = y_3$, $a_5 = y_4$, where the vector $\mathbf{y} = (y_1, y_2, y_3, y_4)^T$ is the solution of the algebraic system $\mathbf{Ey} = \mathbf{b}$, $\mathbf{b} = (0, 2, 0, 0)^T$, $\Delta z_i^* = z_i^* - z_{i-1}^*$ and $\mathbf{E}$ is the matrix:

$$\begin{bmatrix} -(\Delta z_{i-1}^* + \Delta z_i^*) & -\Delta z_i^* & \Delta z_{i+1}^* & (\Delta z_{i+1}^* + \Delta z_{i+2}^*) \\ (\Delta z_{i-1}^* + \Delta z_i^*)^2 & (\Delta z_i^*)^2 & (\Delta z_{i+1}^*)^2 & (\Delta z_{i+1}^* + \Delta z_{i+2}^*)^2 \\ -(\Delta z_{i-1}^* + \Delta z_i^*)^3 & -(\Delta z_i^*)^3 & (\Delta z_{i+1}^*)^3 & (\Delta z_{i+1}^* + \Delta z_{i+2}^*)^3 \\ (\Delta z_{i-1}^* + \Delta z_i^*)^4 & (\Delta z_i^*)^4 & (\Delta z_{i+1}^*)^4 & (\Delta z_{i+1}^* + \Delta z_{i+2}^*)^4 \end{bmatrix}.$$

The first derivative with respect to z^* is approximated as:

$$\frac{\partial C(i,j,k)}{\partial z^*} \approx \delta_z C(i,j,k) = a_1.C(i,j-2,k) + a_2.C(i,j-1,k)$$
$$+ a_3.C(i,j,k) + a_4.C(i,j+1,k) + a_5.C(i,j+2,k),$$

with $a_1 = y_1$, $a_2 = -(y_1 + y_2 + y_3 + y_4)$, $a_3 = y_2$, $a_4 = y_3$, $a_5 = y_4$, where the vector $\mathbf{y}$ is the solution of the algebraic system $\mathbf{Ey} = \mathbf{b}$, here $\mathbf{b} = (1, 0, 0, 0)^T$. The first derivative in the r^* direction is approximated in a similar manner.

The convection–diffusion equation in the drop phase is approximated in a similar way. In order to approximate $\frac{1}{r^*}\frac{\partial}{\partial r^*}\left(r^*\frac{\partial C_d^*}{\partial r^*}\right)$ on the left boundary ($r^* = 0$) we use l'Hospital's Rule: $\lim_{r^*\to 0}\frac{1}{r^*}\frac{\partial C_d^*}{\partial r^*} = \frac{\partial^2 C_d^*}{\partial r^{*2}}$ (see also [27]) and then natural symmetric boundary conditions are imposed.

As it was mentioned, the above described scheme is unstable for $\beta = 0$ (Euler explicit scheme). Thus, two implicit time-stepping schemes were tested: first order implicit, at $\beta = 1$ and second order Crank–Nicolson scheme, at $\beta = 0.5$, see Fig. 2. At $M = 10,000$ Crank–Nicolson scheme ($\beta = 0.5$) is unstable, which indicates that the stable time step for the first order implicit scheme is larger than that when Crank–Nicolson scheme is used. The parameters for this test are: $Pe_d^* = Pe^* = 10^3$; $Pe_s^* = 10^5$; $\lambda^* = 1$; $K^* = K_d^* = \Gamma_{ini}^* = 0.2$, $C_{ini}^* = 1$, $C_{d,ini}^* = 0$. These values of the parameters are chosen to correspond to a more pronounced effect of the surfactant on the film drainage, and at the same time to numerically more challenging situations. Thus at $\lambda^* = 1$ the drainage rate is dominated by the interfacial velocity, u_u^*, (partially-mobile limit, see Fig. 10 of [28]). Note, that the direct effect of the surfactant concentration gradient is on the interfacial velocity via the Marangoni stress, see the second equation (30). The values of the bulk Péclet numbers are chosen for simplicity equal at

Please cite this article in press as: I. Bazhlekov, D. Vasileva, Numerical modeling of drop coalescence in the presence of soluble surfactants, Journal of Computational and Applied Mathematics (2015), http://dx.doi.org/10.1016/j.cam.2015.04.013

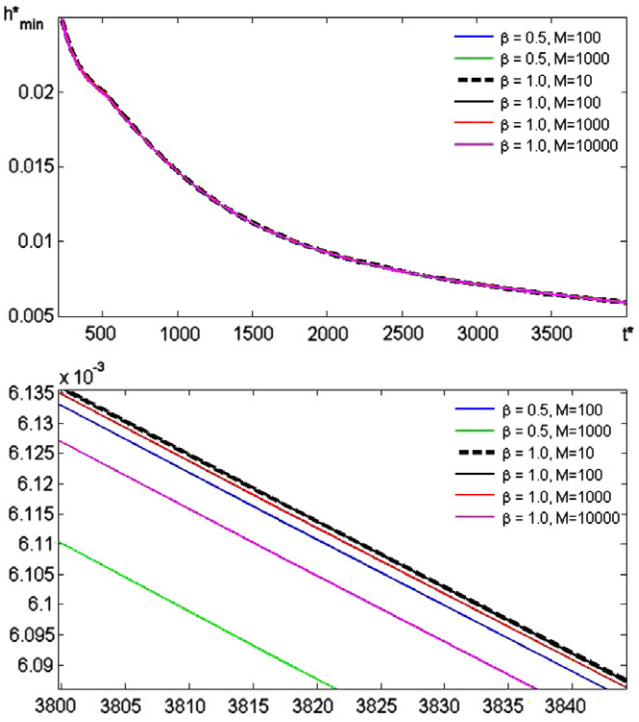

Fig. 2. The evolution of the minimal film thickness h^*_{min} for different time stepping methods.

Table 1
The maximal relative difference RelDiff between the solutions using different time stepping methods and the solution for $\beta = 1, M = 10$.

β	M	RelDiff
1.0	100	$3.0 * 10^{-6}$
1.0	1 000	$0.2 * 10^{-3}$
1.0	10 000	$1.7 * 10^{-3}$
0.5	100	$0.5 * 10^{-3}$
0.5	1 000	$5.0 * 10^{-3}$

an intermediate value of 10^3, see [18]. The surface Péclet number $Pe^*_s = 10^5$ corresponds to a range of negligible diffusion, where the gradients of the surfactant concentration are higher [5] and the simulations are more difficult.

From the first frame of Fig. 2 it is seen that for all values of M considered here the graphs for $h^*_{\min}$ are virtually identical. More detailed inspection (see the second frame of Fig. 2 and also Table 1) indicates that for sufficiently large M the additional error, introduced by the multiple time step integration, is approximately proportional to the value of M. At a given M the results for $\beta = 1$ are an order of magnitude more accurate than that for $\beta = 0.5$. It is also seen from Table 1 that at $\beta = 1, M = 1000$ the additional error is of order 10^{-4}, which is similar to that due to the approximations of the spatial terms ($O(\Delta r^{*2}) \sim 10^{-4}$). Thus, for the simulations presented in the next section the multiple time step integration with $\beta = 1$ and $M = 1000$ is used.

In order to choose an optimal mesh and computational domain number of numerical tests were performed using different space steps (Δz^*_d, $\Delta\eta$ and Δr^*) and computational domains (r^*_l and z^*_∞), see also [22] and [20]. In Fig. 3 the evolution of the minimal film thickness $h^*_{\min}$ and that in the center $h^*_0 = h^*(r^* = 0, t^*)$ are shown for different meshes. In "Base Mesh" the space steps close to the interface ($z^* = h^*/2; z^*_d = 0$) are of order: $\Delta z^*_d \sim 10^{-2}$ in the drop phase and $\Delta z^* \sim 10^{-2}h^*/2$ in the film phase. "Coarse Mesh" is twice coarser and "Fine Mesh" is twice finer than "Base Mesh". Fig. 3 shows that the results for all three meshes are very close regarding the minimal film thickness $h^*_{\min}(t^*)$. For the film thickness in the center of the film, $h^*_0(t^*)$, "Coarse Mesh" does not supply sufficiently accurate results, while the results for the other two meshes are very close. Thus, "Base Mesh" is used for the simulations presented in the next section.

5. Results and discussions

One of the main effects of the insoluble surfactants on drop coalescence is that their presence reduces the film drainage rate (see for instance [5]). The mechanism is schematically shown in Fig. 1: the outward interfacial flow advects the

Please cite this article in press as: I. Bazhlekov, D. Vasileva, Numerical modeling of drop coalescence in the presence of soluble surfactants, Journal of Computational and Applied Mathematics (2015), http://dx.doi.org/10.1016/j.cam.2015.04.013

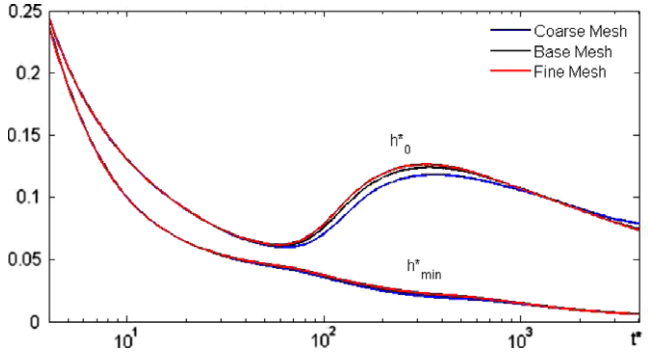

Fig. 3. The evolution of the minimal film thickness h^*_{min} and of the film thickness in the center of the coordinate system h^*_0 for different meshes.

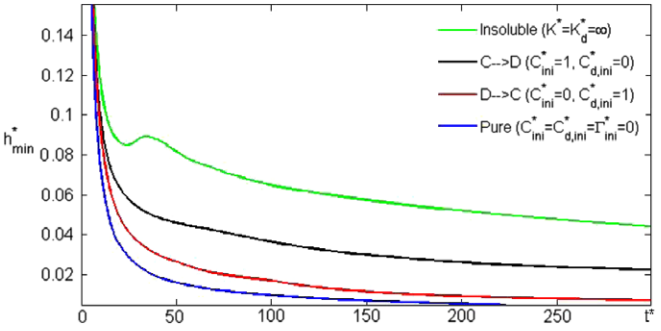

Fig. 4. The evolution of the minimal film thickness h^*_{min} for different limiting cases.

surfactant, generating gradient of the interfacial tension (Marangoni stress) in direction opposite to the flow. The Marangoni stress directly effects the interface velocity u^*_u via the tangential stress τ^*_d and the flow in the drop. Thus the main effect of the surfactant on the film drainage is that it reduces the plug part of the flow towards immobilization of the interface. The method presented in this study can help to understand in detail the influence of surfactants soluble in both phases on the film drainage. To illustrate this in the present section two limiting cases of the initial surfactant distribution are considered, see the conditions (43) and (44): $(D \to C)$—initially the surfactant is uniformly distributed only in the drop phase at $C^*_{d,ini} = 1;\ C^*_{ini} = 0$; $(C \to D)$—initially the surfactant is uniformly distributed only in the film phase at $C^*_{d,ini} = 0;\ C^*_{ini} = 1$. The other parameters are kept the same: $Pe^*_d = Pe^* = 10^3;\ Pe^*_s = 10^5;\ \lambda^* = 1;\ K^* = K^*_d = \Gamma^*_{ini} = 0.2$.

Fig. 4 shows the evolution of the minimal film thickness, $h^*_{\min}$ for the above mentioned initial conditions ($C \to D$ and $D \to C$). The results are compared with the cases of film drainage in the presence of an insoluble surfactant and that for a pure system (in absence of surfactants). For both cases ($C \to D$ and $D \to C$) the film drainage is faster than that for the insoluble surfactant and slower than that for the pure system. It is also seen that in the case of initial surfactant transport from the drop to the continuous (film) phase ($D \to C$) the film drainage is faster than that when the transfer is in the opposite direction ($C \to D$). This situation is similar to that of inter-phase mass transfer, see [18,20]. In contrast to the present results the ($D \to C$) inter-phase mass transfer leads to film drainage faster than that for "Pure" case. The difference is due to the presence of surfactants on the interface, which leads towards immobilization of the interfaces and respectively slower film drainage.

For a better understanding of the effect of soluble surfactants on the drainage rate of the film in Figs. 5 and 6 the distribution of the surfactant concentration is presented at several time instances. In order to analyze qualitatively the possible effects of the surfactant on the film drainage, different processes can be considered: First, due to the exchange of the surfactant between the phases, boundary layers of the surfactant concentration are formed at both sides of the interfaces. Second, with the progressing film drainage, the surfactant on the interface is advected outwards the film center, creating a significant gradient of the surfactant concentration on the interface. Third, the exchange of the surfactant between the interface and the surrounding bulk phases in general decreases the gradients of the surfactant on the interface.

The interplay of the above described subprocesses of the surfactant transport effects the Marangoni stress and in this way the film drainage. The thickness of the boundary layers increases with time, while the thickness of the film decreases. Thus, when the thickness of the boundary layer in the film phase becomes comparable with the half thickness of the film, the two boundary layers overlap in the region where the film thickness is minimal. In the case $D \to C$, Fig. 5, this is seen after the second frame. Indeed, at time $t^* = 44.8$ (see the third frame of Fig. 5) the concentration at the periphery of the film, around $r^* = 1.2$, is the highest. The distribution of the surfactant concentration Γ^* on the interfaces is similar, highest just outside the film. Having in mind, that the Marangoni stress is proportional to $-\nabla\Gamma^*$, it can be concluded that such

Please cite this article in press as: I. Bazhlekov, D. Vasileva, Numerical modeling of drop coalescence in the presence of soluble surfactants, Journal of Computational and Applied Mathematics (2015), http://dx.doi.org/10.1016/j.cam.2015.04.013

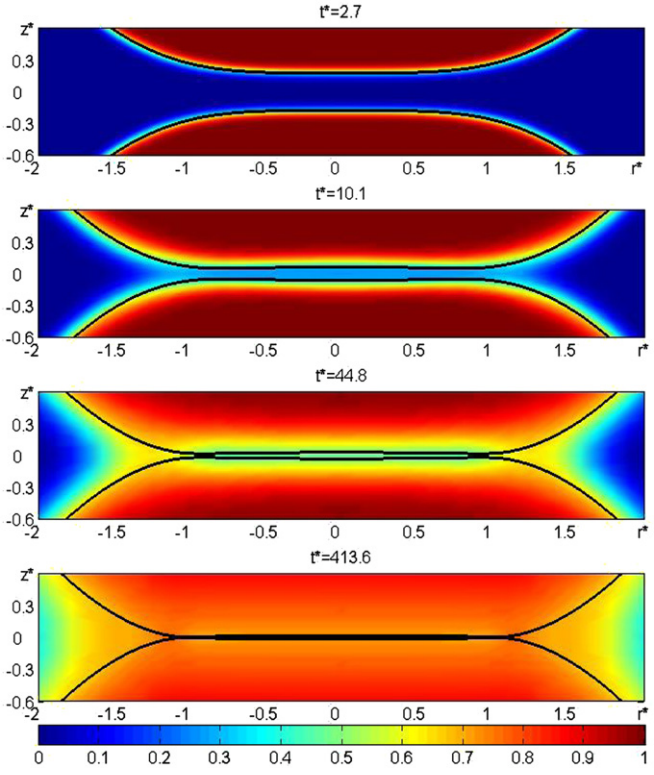

Fig. 5. The surfactant distribution in the drop and in the film at four time instances for $C^*_{d,ini} = 1$; $C^*_{ini} = 0$.

surfactant distribution promotes the local film drainage. A similar effect is seen in the case of inter-phase mass transfer (see [20]) when the transfer of solutes is from the drop to the continuous phase.

The surfactant distribution in the opposite case $C \to D$ (when initially the surfactant is only in the continuous phase) is shown in Fig. 6 for five time instances. In this case the advection of the surfactant on the interfaces and the surfactant transport from the continuous to the drop phase act in one and the same direction, decreasing the surfactant concentration in the film region and adjacent parts of the interfaces. Thus, after time $t^* = 60.3$ (see the third frame of Fig. 6) the film region is exhausted from the surfactant while the concentration in the continuous phase outside the film region ($r^* > 1.5$) is still high. Such distribution of the surfactant concentration in the film, and respectively on the interface, generates Marangoni stress in direction opposite to the film drainage. This explains the slower (about 10 times) film drainage, compared with that in the case ($D \to C$). Let us analyze the contribution of the Marangoni stress in the total stress τ^*_d, see Eq. (30). It is seen from Eq. (28) that the hydrodynamic part of the stress, τ^* is proportional to the film thickness h^*. The film thickness decreases with time and for $t^* = 60.3$ is of order $h^* \sim 5 * 10^{-2}$, see Fig. 7. Thus, at this stage of the film drainage, the Marangoni stress dominates over the hydrodynamic one, resulting in a negative total stress $\tau^*_d < 0$. This generates, via the flow in the drops, negative interface velocity, leading to an increase of the film thickness in the center, see Fig. 7.

The effect of the van der Waals forces (disjoining pressure) on the film rupture is shown in Fig. 8 in the case $C \to D$, and for the same values of the parameters. It is seen that at the last stage of the film drainage the thickness of the film decreases to values at which the intermolecular van der Waals forces become significant. Being proportional to h^{*-3} (see the last term in (32)) once the van der Waals forces are comparable with the other forces they become dominant very fast leading to film rupture. This is seen in Fig. 8 at different values of the transformed Hamaker parameter A^*. At this stage the last limitation in (46) on the time step ($(\Delta t^*)_{III}$) becomes most restrictive, limiting the time steps to values of order $\Delta t^* \sim 10^{-9}$ and even smaller.

6. Conclusions

A numerical method is presented for simulation of film drainage between axisymmetrically interacting drops in the presence of a surfactant soluble in both, drop and film, phases. The mathematical model includes fully coupled flow and concentration equations in both phases as well as on the interface. The presented tests, comparisons and numerical experiments show that the method is capable to simulate drainage of films with thickness of order of the critical film thickness. The intermolecular van der Waals forces are also considered. They become dominant at the last stage of the film drainage, predicting the film rupture and a consequential coalescence. Different approaches for optimization of the numerical algorithm are tested: Non-uniform meshes for space discretization in the film and drop phases; Time integration schemes with

Please cite this article in press as: I. Bazhlekov, D. Vasileva, Numerical modeling of drop coalescence in the presence of soluble surfactants, Journal of Computational and Applied Mathematics (2015), http://dx.doi.org/10.1016/j.cam.2015.04.013

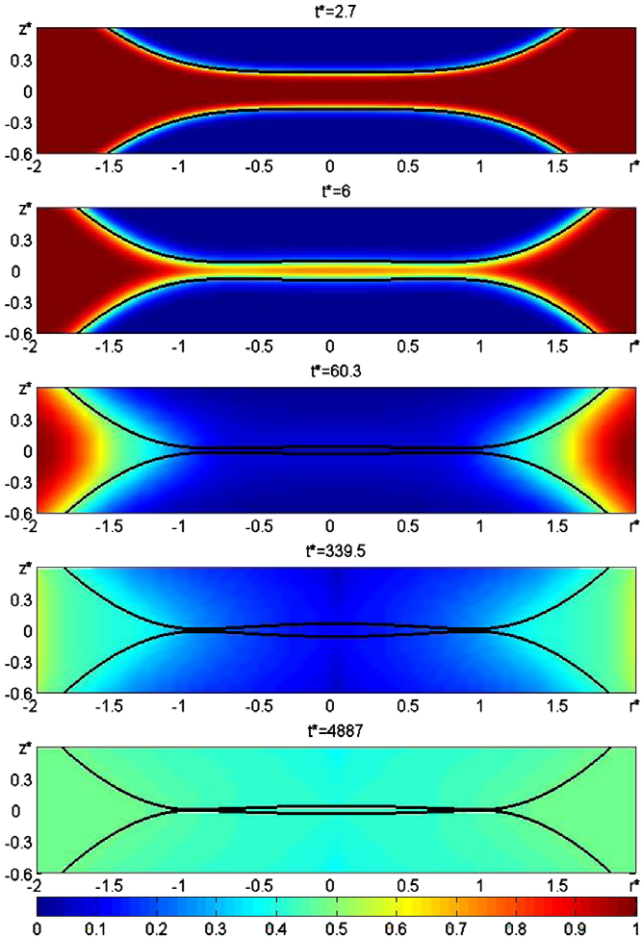

Fig. 6. The surfactant distribution in the film and in the drop at five time instances for $C^*_{d,ini} = 0$; $C^*_{ini} = 1$.

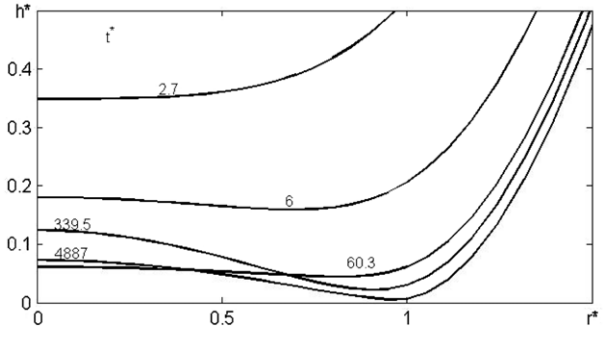

Fig. 7. The evolution of the film thickness h^* for $C^*_{d,ini} = 0$; $C^*_{ini} = 1$.

automatically adaptive time steps; A multiple time step integration scheme that can improve significantly the performance of the computations; A hybrid (explicit/implicit) method is developed for time integration of the convection–diffusion equations in the drop and film phases, which consists of explicit time integration in the r^* direction and implicit in the z^* (z^*_d) direction. The presented numerical method will be used in a following study for a more extensive investigation of the effect of soluble surfactants on the drop coalescence, where practically interesting values of the parameters will be considered.

Acknowledgments

The authors are partially supported by Grant DFNI-I02/9/12.12.2014 from the Bulgarian National Science Fund. The authors would like to thank the referees for their valuable comments and suggestions.

Please cite this article in press as: I. Bazhlekov, D. Vasileva, Numerical modeling of drop coalescence in the presence of soluble surfactants, Journal of Computational and Applied Mathematics (2015), http://dx.doi.org/10.1016/j.cam.2015.04.013

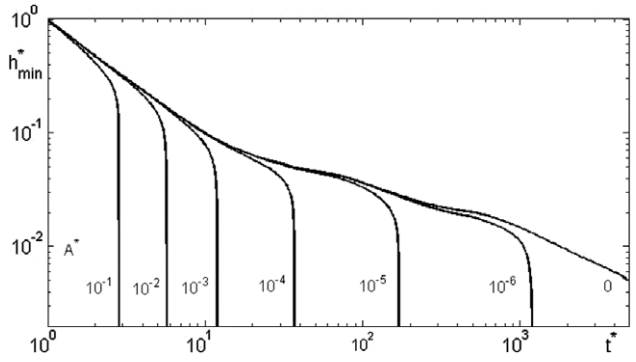

Fig. 8. The evolution of the minimal film thickness h^*_{min} for different values of the Hamaker constant A^*.

References

[1] S.N. Maindarkar, N.B. Raikar, P. Bongers, M.A. Henson, Incorporating emulsion drop coalescence into population balance equation models of high pressure homogenization, Colloids Surf. A 396 (2012) 63–73.
[2] N. Kopriwa, F. Buchbender, J. Ayesterán, M. Kalem, A. Pfennig, A critical review of the application of drop-population balances for the design of solvent extraction columns: I. Concept of solving drop-population balances and modelling breakage and coalescence, Solvent Extr. Ion Exch. 30 (2012) 683–723.
[3] H.A. Stone, L.G. Leal, Effects of surfactants on drop deformation and breakup, J. Fluid Mech. 220 (1990) 161–186.
[4] A. Chesters, Modelling of coalescence processes in fluid-liquid dispersions. A review of current understanding, Chem. Eng. Res. Des. 69 (1991) 259–270.
[5] A. Chesters, I. Bazhlekov, Effect of insoluble surfactants on drainage and rupture of a film between drops interacting under a constant force, J. Colloid Interface Sci. 230 (2000) 229–243.
[6] A.F. Jones, S.D.R. Wilson, Film drainage problem in droplet coalescence, J. Fluid Mech. 87 (1978) 263–288.
[7] Dongming Li, Coalescence between two small bubbles or drops, J. Colloid Interface Sci. 163 (1994) 108–119.
[8] A. Saboni, C. Gourdon, A. Chesters, Drainage and rupture of partially mobile films during coalescence in liquid–liquid systems under a constant interaction force, J. Colloid Interface Sci. 175 (1995) 27–35.
[9] M.B. Nemer, Near-contact motion of liquid drops in emulsions and foams (Ph.D. thesis), Yale University, USA, 2003.
[10] P. Santoro, M. Loewenberg, Coalescence of drops with tangentially mobile interfaces: Effects of ambient flow, Ann. New York Acad. Sci. 1161 (2009) 277–291.
[11] M.B. Nemer, P. Santoro, X. Chen, J. Blawzdziewicz, M. Loewenberg, Coalescence of drops with mobile interfaces in a quiescent fluid, J. Fluid Mech. 728 (2013) 471–500.
[12] K.D. Danov, D.S. Valkovska, I.B. Ivanov, Effect of surfactants on the film drainage, J. Colloid Interface Sci. 211 (1999) 291–303.
[13] D.S. Valkovska, K.D. Danov, I.B. Ivanov, Effect of surfactants on the stability of films between two colliding small bubbles, Colloids Surf. A 175 (2000) 179–192.
[14] L.Y. Yeo, O.K. Matar, E.S. Perez de Ortiz, G.F. Hewitt, Film drainage between two surfactant-coated drops colliding at constant approach velocity, J. Colloid Interface Sci. 257 (2003) 93–107.
[15] B. Dai, L.G. Leal, The mechanism of surfactant effects on drop coalescence, Phys. Fluids 20 (2008) 040802.
[16] J. Blawzdziewicz, E. Wajnryb, M. Loewenberg, Hydrodynamic interactions and collision efficiencies of spherical drops covered with an incompressible surfactant film, J. Fluid Mech. 395 (1999) 29–59.
[17] K. Danov, S. Stoyanov, N. Vitanov, I. Ivanov, Role of surfactants on the approaching velocity of two small emulsion drops, J. Colloid Interface Sci. 368 (2012) 342–355.
[18] A. Saboni, C. Gourdon, A. Chesters, The influence of inter-phase mass transfer on the drainage of partially-mobile liquid films between drops undergoing a constant interaction force, Chem. Eng. Sci. 54 (1999) 461–473.
[19] A. Saboni, S. Alexandrova, C. Gourdon, A.K. Chesters, Interdrop coalescence with mass transfer: Comparison of the approximate drainage models with numerical results, Chem. Eng. J. 88 (2002) 127–139.
[20] I. Bazhlekov, D. Vasileva, Numerical simulation of drop coalescence in the presence of inter-phase mass transfer, in: Lecture Notes in Comput. Sci., vol. 8962, 2015, pp. 237–245.
[21] I. Bazhlekov, Numerical simulation of drop coalescence in the presence of film soluble surfactant, AIP Conf. Proc. 1487 (2012) 351–359.
[22] I. Bazhlekov, D. Vasileva, Numerical simulation of drop coalescence in the presence of drop soluble surfactant, AIP Conf. Proc. 1561 (2013) 333–346.
[23] K. Jansons, J. Lister, The general solution of Stokes flow in a half space as an integral of the velocity on the boundary, Phys. Fluids 31 (1988) 1321–1323.
[24] O. Ladyzhenskaya, The Mathematical Theory of Viscous Incompressible Flow, in: Mathematics and its Applications, vol. 2, Gordon and Breach Science Publishers, New York, 1969.
[25] M. Rother, A. Zinchenko, R. Davis, Buoyancy-driven coalescence of slightly deformable drops, J. Fluid Mech. 346 (1997) 117–148.
[26] I. Bazhlekov, F. van de Vosse, Multiple time step approach for numerical simulation of non-Newtonian drop coalescence, in: O.P. Iliev, M.S. Kaschiev, S.D. Margenov, Bl.H. Sendov, P.S. Vassilevski (Eds.), Recent Advances in Numerical Methods and Applications, World Scientific, Singapore, 2009, pp. 773–781.
[27] A.A. Samarskii, The Theory of Difference Schemes, CRC Press, 2001.
[28] I. Bazhlekov, F. Vosse, A. Chesters, The effect of the dispersed to continuous-phase viscosity ratio on film drainage between interacting drops, Int. J. Multiphase Flow 26 (2000) 445–466.

Please cite this article in press as: I. Bazhlekov, D. Vasileva, Numerical modeling of drop coalescence in the presence of soluble surfactants, Journal of Computational and Applied Mathematics (2015), http://dx.doi.org/10.1016/j.cam.2015.04.013